Journal of Research in Science and Engineering (JRSE)
ISSN: 1656-1996 Volume-8, Issue-5, May 2026
DOI: 10.53469/jrse.2026.08(05).08

Injury of Average-sized Female Pedestrians in Vehicle Collisions

Xiaoye Huo, Shihai Cui

Tianjin University of Science and Technology, Tianjin 300457, China

Abstract: ***Objective:*** ***To investigate the influence of initial pedestrian motion states on the injury outcomes of average-sized female pedestrians in vehicle-pedestrian collisions.*** ***Methods:*** ***A biofidelic injury model of the Average-sized female pedestrian was developed, and a pedestrian-vehicle collision simulation platform was established. Simulations were conducted under two pedestrian walking speeds (0 and 5 km/h) and a vehicle impact speed (40 km/h) across multiple scenarios to explore the injury mechanisms of Average-sized female pedestrians during the collision process.*** ***Results:*** ***The results indicate that pedestrian gait exerts a non-linear influence on injury patterns under these two typical collision conditions. Ligament ruptures in the lower limbs were observed in both scenarios. Notably, the pedestrian with an initial velocity exhibited the highest Brain Injury Criterion (BrIC) value, suggesting a significantly higher risk of Diffuse Axonal Injury (DAI).*** ***Conclusion:*** ***Incorporating initial pedestrian kinetic energy into simulations provides a more realistic representation of the biomechanical collision process. The findings offer refined biomechanical references for the passive safety design of vehicles targeting female pedestrians in China.***

Keywords: a Average-sized female, Pedestrian injury model with high biofidelity, Collision simulation, Biomechanical response**.**

1. Introduction

According to the 2023 report by the World Health Organization (WHO), it is estimated that road traffic fatalities reached 1.19 million in 2021, marking a 5% decrease compared to previous benchmarks. Road traffic collisions remain a leading global cause of mortality, with the protection of Vulnerable Road Users (VRUs), particularly pedestrians, presenting an especially urgent challenge [1]. This issue is particularly pronounced in China, where the typical “mixed traffic” paradigm further complicates the road safety environment. On Chinese roadways, motorized vehicles, non-motorized vehicles (specifically the large-scale integration of electric bicycles), and pedestrians frequently coexist within the same space over long distances, leading to pervasive right-of-way conflicts. In such complex environments, pedestrians suffer from a significantly higher casualty rate than other groups due to their lack of physical protection, positioning them as a primary critical vulnerability in traffic safety. Furthermore, the interplay of intricate road conditions, varying levels of safety awareness, and diverse driving behaviors contributes to the occurrence of various collision typologies [2].

In China’s road traffic accidents, motor vehicle violations account for 86.29% of the total, with failure to yield right-of-way being a primary factor. Furthermore, multi-vehicle accidents constitute 70.21% of all cases, with side-impact collisions identified as the predominant configuration [3]. Analysis of pedestrian accident data in Japan from 1999 to 2009 by Matsui et al. [4] demonstrated that traumatic brain injury (TBI) remains the leading cause of pedestrian fatalities, with a higher mortality rate observed among females than males. Zhang et al. [5] conducted pedestrian-vehicle collision (PVC) simulations using a Average-sized male pedestrian model across various impact orientations. With the pedestrian model set in a stationary position, the results indicated that variations in the impact location significantly influence the transmission paths and energy distribution of the impact, leading to marked changes in injury patterns and mechanisms. Based on 181 fatal pedestrian cases from the National Automotive Accident In-depth Investigation System (NAIS), Zhang et al. [6] pointed out that illegal road crossing is the primary cause of pedestrian death. Their findings revealed that over half of the collisions occurred in the center-front or slightly offset regions, while 43.6% were located at the front corners. During a collision, the significant disparity in mass and momentum often causes the pedestrian to undergo a primary impact with the vehicle followed by a secondary impact with the ground after being projected into the air; both stages can result in severe injuries. Zhao et al. [7] developed a biofidelic injury model for small-stature female pedestrians with detailed anatomical structures tailored to Chinese anthropometry. Evaluations based on the Euro NCAP CP540 standard showed that the model’s responses remained within regulatory corridors, exhibiting excellent biomechanical fidelity. Additionally, Zhang et al. [8] utilized the THUMS model to reconstruct collisions for lower-limb kinetic response and injury analysis. The results showed that the transverse structural characteristics of the vehicle’s front end significantly affect the kinematic response and injury of the pedestrian’s legs, where lateral bending angles and shear displacements at the knee joint are more likely to induce ligament strains and dislocations.

In summary, current domestic and international biomechanical studies on pedestrian injuries predominantly focus on male subjects or small-stature females, while research specifically targeting mid-sized female pedestrians remains scarce. Therefore, this study focuses on mid-sized females and utilizes numerical simulations to investigate their injury mechanisms and biomechanical responses during pedestrian-vehicle collisions.

2. Experimental Setup

2.1 Pedestrian Model Selection

To obtain more realistic data for average-sized females, a human body model was developed and validated using Mimics, Geomagic, and ANSA software, following the

modeling methodology of Zhao, H. et al. [7]. Consequently, a biofidelic standing posture model for injury analysis of the Average-sized female pedestrian was established. This model incorporates detailed anatomical structures, including the brain tissue, internal organs, muscles, ligaments, bones, skin, and fat.

During the modeling process, given that mesh quality significantly affects subsequent computational stability [8], hexahedral and shell elements were primarily utilized to enhance the model's stability and convergence performance. The interconnections between various anatomical structures were achieved through common node connections and single-surface contact definitions, effectively ensuring the consistency of mechanical transmission. The material properties of the biological tissues were defined based on relevant literature [9-16]: ligaments were modeled as elastoplastic materials, muscles as linear elastic, fat and internal organs as viscoelastic, and skin as elastic. Finally, the validity of the model was verified against published cadaveric test data.

2.2 Collision Simulation Setup

A vehicle-pedestrian collision simulation platform was constructed based on the established pedestrian model and a sedan finite element (FE) model (Honda Accord) released by the National Crash Analysis Center (NCAC) [17]. To balance computational efficiency and simulation stability, the sedan model was reasonably simplified: components not directly involved in collision contact were removed, and equivalent mass points were assigned at the vehicle's center of gravity and relevant nodes to accurately preserve its mass distribution characteristics.

To systematically investigate pedestrian injury responses, the vehicle impact speed was set to 40 km/h, in accordance with the speed limit regulations for different road classes in Article 45 of the Road Traffic Safety Law of the People's Republic of China [18]. Meanwhile, the median value of 5 km/h, within the typical adult walking speed range (4–6 km/h), was selected as the initial pedestrian velocity. Two comparative test groups were established with initial speeds of 0 km/h (stationary) and 5 km/h (normal speed). The total simulation duration was set to 500 ms to fully capture the kinematic response process of the pedestrian post-impact.

3. Results and Analysis

3.1 Analysis of Pedestrian Kinematic Response

In the stationary condition, the kinematic response of the pedestrian begins with the vehicle bumper first impacting the lower limbs, causing significant deformation of the knee joints under the combined effects of shear force and inertia. As the collision progresses, secondary contact occurs between the pedestrian's pelvis and thigh regions and the leading edge of the vehicle hood. Due to the rapid acceleration of the lower limbs in the direction of the vehicle's motion, while the torso lags behind due to inertia, a strong rotational moment is generated around the front edge of the vehicle. This results in a typical "wrap-around motion" (WAM) pattern. During this phase, both feet leave the ground, and the body rotates around the front of the vehicle, with the arms flailing in a projectile-like manner due to centrifugal force. In the later stages of the collision, the body continues to move outward and upward under the influence of rotation. The wide-ranging projectile motion of the arms reflects an instinctive protective response in a weightless state and a complex spatial trajectory. Ultimately, the pedestrian's head, acting as the distal end of the kinetic chain, strikes the rear part of the hood. The kinematic parameters of the head strike directly influence the Head Injury Criterion (HIC), serving as a critical basis for evaluating the head protection capabilities of the vehicle's front-end structure.

The primary difference between the condition with initial kinetic energy and the stationary condition lies in the initial stage of the simulation. At the onset, the pedestrian model is assigned an initial velocity, exhibiting a clear forward-walking trend within a short duration. Under the influence of gravity and the initial velocity vector, the model undergoes a dynamic self-balancing process, achieving a stable gait transition from the left foot lifting to touching the ground, accurately replicating a normal walking posture. Subsequently, its kinematic response aligns with that of the stationary condition. This high-fidelity pre-collision kinematic simulation ensures that the model is in a realistic gait phase at the moment of impact, establishing a biomechanical foundation for analyzing subsequent kinematic responses under collision loads.

3.2 Head Injury Assessment

In pedestrian-vehicle collision (PVC) simulations, head injury assessment primarily refers to the Head Injury Criterion (HIC15), the Brain Injury Criterion (BrIC), and the probability of AIS 4+ injury, P (AIS 4), derived from BrIC. Analysis of the simulation data at a vehicle speed of 40 km/h shows that the HIC15 value for the stationary pedestrian condition is 664.5, while it is 611 for the condition with initial kinetic energy. Variations in pedestrian movement speed exert a significant influence on head injury indices. Specifically, the HIC15 value in the stationary condition is higher than that in the moving condition, indicating that walking speed affects pedestrian injury during the collision. Although the HIC15 values are below the conventional injury threshold of 700 [19], the associated risks of skull fracture and concussion are significantly elevated, suggesting that such collisions can still cause severe or even fatal head injuries. Pedestrian walking speed alters the relative contact position and impact angle between the head and the vehicle. When the pedestrian has an initial velocity, the BrIC value is 1.09, corresponding to a P (AIS 4) probability of 0.41; when stationary, the BrIC value is 0.96, while the P (AIS 4) value rises to 0.53. It is generally accepted that brain tissue faces a high injury risk when BrIC > 1.0 [20]. These results indicate that the momentum superposition effect becomes more pronounced when pedestrians collide with vehicles at higher speeds, leading to a sharp increase in injury risk. From the perspective of biomechanical protection, it is recommended that pedestrians strictly adhere to traffic signals, particularly avoiding illegal rushing during the transition between yellow and red lights, to mitigate the potential risk of high-intensity collision injuries caused by "accelerated sprinting."

In the pedestrian-vehicle collision simulation scenarios, the Von Mises stress and shear stress within the brain tissue of the pedestrian model were investigated. Comparing the stress distributions between the stationary and moving states, it was observed that in the stationary condition, the peak Von Mises stress and shear stress were 14.75 kPa and 8.51 kPa, respectively. In contrast, under the condition with an initial walking speed, the Von Mises stress was 12.04 kPa and the shear stress was 7.063 kPa. These findings indicate that the introduction of walking velocity alters the impact location, subjecting the brain tissue to more complex compressive and shearing effects, which ultimately leads to distinct injury outcomes.

Furthermore, the intracranial pressure (ICP) and maximum principal strain (MPS) of the pedestrian model were analyzed. Comparing the ICP responses between the stationary and moving states, the peak ICP in the stationary condition was 327 kPa. Upon introducing walking speed, the peak ICP reached 428.7 kPa at 5 km/h; at this level, brain tissue is likely to sustain severe injuries such as cerebral contusion, laceration, and intracranial hematoma. The MPS reflects the degree of internal tensile deformation in brain tissue and serves as a critical indicator for assessing the risk of Diffuse Axonal Injury (DAI). It is generally accepted that the risk of DAI increases significantly when the strain in brain tissue exceeds 0.15 to 0.20. Comparing the strain distribution of the pedestrian in stationary versus moving states, the stationary condition exhibited the smallest area of high-strain regions. With an initial velocity, the areas of strain concentration in the cerebral cortex and deep tissues expand, indicating that pedestrian motion significantly intensifies the rotational and tensile deformation of the brain tissue. As Average-sized females have relatively weak cervical musculature, providing limited constraint against head rotation and stretching, their strain response is highly sensitive to walking speed. Consequently, an increase in walking speed markedly exacerbates the strain response of the brain tissue, thereby elevating the risk of DAI.

In conclusion, the comparative mechanical analysis of brain tissue demonstrates that walking speed significantly influences craniocerebral injury patterns in pedestrian-vehicle collisions. Relying exclusively on stationary conditions for assessment underestimates the actual risk of severe injury in real-world traffic environments. Consequently, the impact of pedestrian motion on the biomechanical response of craniocerebral collisions should be further integrated into the development and evaluation of vehicle active safety systems to enhance the predictive accuracy of pedestrian injuries in real accident scenarios.

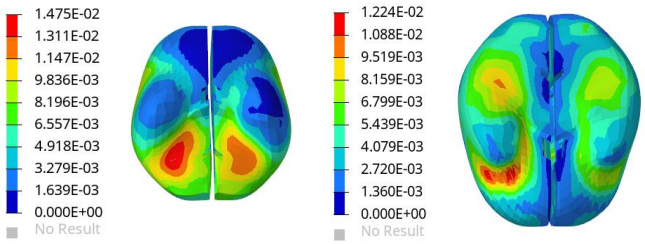

Von Mises Stress Contour Plot

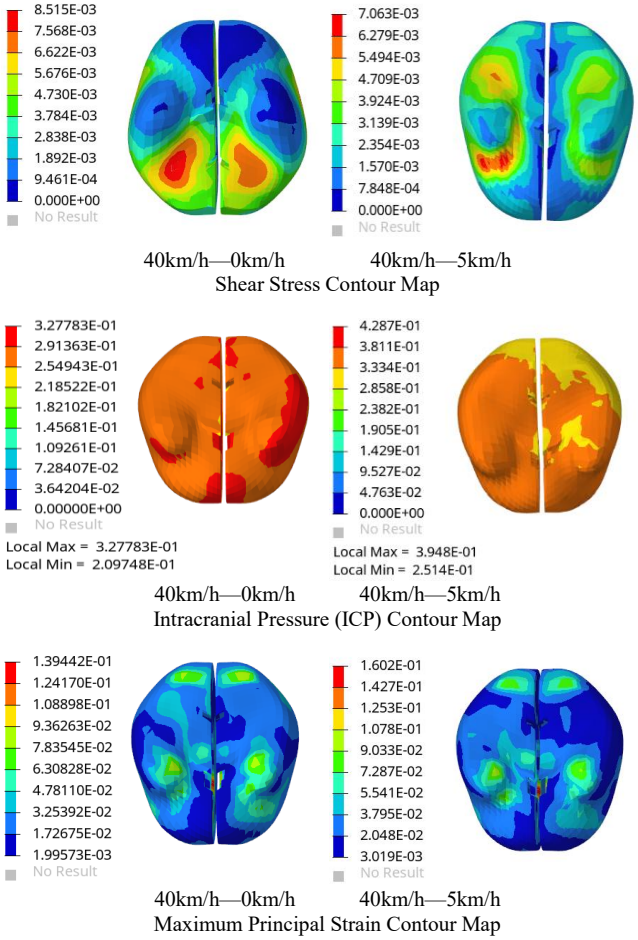

Maximum Principal Strain Contour Map

Figure 1: Stress Contour Map of Pedestrian-Vehicle Collision

3.3 Lower Limb Injury Analysis

Comparing the kinematic responses of the simulation tests, it was observed that the primary impact location during the initial collision phase was the lateral side of the right knee joint, a result heavily influenced by the pedestrian's stature and physical characteristics. Simulation data revealed that ligament ruptures of varying severity occurred simultaneously across all test cases (see Table 2).

Beyond macroscopic failure, a detailed analysis of the Von Mises stress and shear stress in the tibia and fibula was conducted. The peak stresses in the stationary condition were slightly lower than those in the moving condition. This suggests that walking speed significantly influences lower limb injury outcomes, primarily by altering the limb posture at the moment of impact. Variations in velocity lead to different contact orientations, placing the tibia in a more vulnerable loading angle or support state, which intensifies stress concentration.

From a kinematic perspective, the Average-sized female model primarily sustains impact at the lateral knee, leading to catastrophic ligamentous rupture, particularly in the ACL and MCL. Although stress contour maps primarily visualize surface loading, the underlying data indicates a high risk of bone contusions (bone bruises). The peak Von Mises stresses in the tibia and fibula reached 123–124 MPa, critically approaching the cortical bone strength limit of 125 MPa. This proximity to the mechanical threshold, combined with rapid

loading rates, suggests that while a complete fracture may not be explicitly captured on the surface mesh, internal trabecular micro-damage and subchondral bone bruising are highly likely, posing a severe risk of occult injury.

Table 2: Pedestrian-Vehicle Collision Ligament Rupture Moment

Left leg ligament	Injury Outcomes	Right leg ligament	Injury Outcomes
MCL	Undamaged	MCL	144ms
LCL	154ms	LCL	Undamaged
ACL	149ms	ACL	134ms
PCL	Undamaged	PCL	139ms

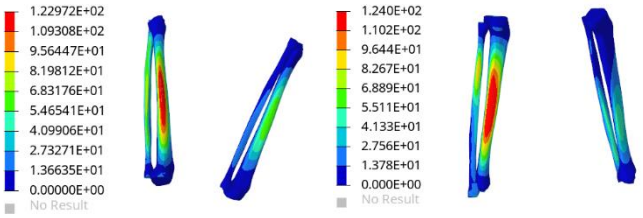

Figure 2: Von Mises Stress Contours of the Pedestrian Tibia and Fibula in Pedestrian-Vehicle Collision

In summary, the comparative analysis of the biomechanical responses of Average-sized females at varying pedestrian speeds reveals the complex influence of initial motion states on injury mechanisms. While traditional crash simulations typically employ a stationary state to represent pedestrian posture at the moment of impact, the findings of this study highlight the inherent limitations of this simplified approach in evaluating pedestrian-vehicle collision injuries. At a standard walking speed of 5 km/h, the head HIC15 value and peak intracranial pressure (ICP) did not exhibit a significant increase compared to the stationary condition; conversely, localized decreases were observed. From a biomechanical perspective, this non-linear fluctuation is primarily attributable to the alteration of impact dynamics by the gait phase. The walking motion shifts the pedestrian's center of gravity forward, thereby modifying the Wrap-Around Distance (WAD) of the head-vehicle contact and allowing the head to avoid certain high-stiffness components beneath the hood. Furthermore, the cushioning effect provided by the lower limbs in a dynamic posture partially delays energy transmission to the head. This suggests that under normal walking conditions, the modification of the impact posture serves as a subtle force-mitigation (load-shedding) mechanism in the short term.

4. Conclusion

A pedestrian simulation model was developed based on the anthropometric data of Average-sized female pedestrians, and a comprehensive pedestrian-vehicle collision research platform was established. This study investigated the biomechanical injury responses under coupled impact scenarios involving a vehicle speed of 40 km/h and pedestrian walking speeds of 0 km/h and 5 km/h. Based on the analysis of pedestrian kinematic responses and biomechanical injury indices of critical body regions, the following conclusions were reached:

1) Pedestrian walking speed exerts a significant influence on the injuries sustained by Average-sized females. Compared with the stationary condition (0 km/h), walking at a low speed of 5 km/h alters the collision wrap-around trajectory and the subsequent head impact location. The gait posture provides a certain buffering effect during the initial stage of the collision, leading to a transient reduction in translational head injury metrics and localized intracranial pressure (ICP). This indicates that assessments relying exclusively on stationary conditions may lead to a misinterpretation of compression injury characteristics in low-speed dynamic scenarios.

2) Pedestrian walking speed exerts a non-linear modulation on injury responses. By altering the body posture at the moment of impact, the walking velocity significantly influences the biomechanical loading mechanisms of both the lower limbs and the head. In the 5 km/h walking scenario, the momentum superposition of the vehicle and the pedestrian leads to a substantial increase in BrIC and maximum principal strain (MPS). This indicates that high-speed walking behaviors common in real-world traffic, such as "rushing," expose pedestrians to a heightened risk of diffuse axonal injury (DAI).

References

[1] Global status report on road safety 2023 [J]. Health and Safety, 2023 (Dec.18):15-16

[2] Berfenstam R. Sweden's pioneering child accident programme: 40 years later. [J]. Injury Prevention, 1995, 1 (2):68-69.

[3] Gao, Y. N., & Gong, J. Q. (2023). Analysis of characteristics and causes of road traffic accidents in China. Journal of Safety and Environment, 23 (11), 4013–4023. https://doi.org/10.13637/j.issn.1009-6094.2022.1844

[4] Matsui, Yasuhiro, et al. "Features of Fatal Pedestrian Injuries in Vehicle-to-Pedestrian Accidents in Japan." SAE International Journal of Transportation Safety, vol. 1, no. 2, 2013, pp. 297–308. JSTOR, http://www.jstor.org/stable/26169224. Accessed 16 Mar. 2026.

[5] C. M. Zhang, "Development and application research of a biofidelic injury model for the 50th percentile Chinese male pedestrian," Master's thesis, Tianjin University of Science and Technology, 2024. doi: 10.27359/d.cnki.gtqgu.2024.000639.

[6] S. B. Zhang, L. Liu, P. F. Li, et al., "Research on characteristics and causal mechanisms of pedestrian fatal traffic accidents: Based on 181 deeply investigated accident cases," Traffic Information and Safety, vol. 36, no. 06, pp. 16–23, 2018.

[7] Zhao, H., Li, H., Wang, Y. (2026). Development of a 5th percentile Chinese female pedestrian injury bionic model and certification in accordance with Euro NCAP CP540. Computer Methods in Biomechanics and Biomedical Engineering, 1–11. https://doi.org/10.1080/10255842.2026.2635692

[8] D. W. Zhang, Y. Lei, Y. Ren, et al., "Kinetic response and injury biomechanics analysis of pedestrian lower limbs based on pedestrian-vehicle collision accident reconstruction," Journal of Automotive Safety and Energy, vol. 14, no. 06, pp. 671–680, 2023.

[9] Katcher M L, Bull M J, Palmer S D, et al. Selecting and Using the Most Appropriate Car Safety Seats for Growing Children: Guidelines for Counseling Parents [J]. Pediatrics, 2002, 109 (3):550-553.
[10] Philippe B, Paul C B, King H Y, et al. Lower Limb: Advanced FE Model and New Experimental Data [J]. Stapp Car Crash Journal, 2001, 45 (12):1-25.
[11] Untaroiu C K, Darvish J C, Deng B, et al.A finite element model of the lower limb for simulating pedestrain impacts [J]. Stapp Car Crash Journal, 2005, 41 (3):157-181.
[12] Miller K, Chinzei K. Constitutive modelling of brain tissue: experiment and theory [J]. Journal of Biomechanics, 1997, 30 (11-12):1115-1121.
[13] Miller-Young J E, Duncan N A, Baroud G. Material properties of the human calcaneal fat pad in compression: experiment and theory [J]. Journal of Biomechanics, 2002, 35 (12):1523-1531.
[14] Wang HK. Development of a side impact finite element human thoracic model
[15] Ruan J S, El-Jawahri R, Barbat S, et al. Biomechanical Analysis of Knee Impact in Frontal Collisions through Finite Element Simulations with a Full Human BodyModel [J]. Sae Technical Papers, 2008 [D]. Detroit: Wayne State University, 1995.
[16] Ruan J, El-Jawahri R, Chai L, Barbat S, Prasad P. Prediction and analysis of human thoracic impact responses and injuries in cadaver impacts using a full human body finite element model. Stapp Car Crash J. 2003 Oct; 47: 299-321. doi: 10.4271/2003-22-0014. PMID: 17096254.
[17] National Crash Analysis Center. Finite element model archive [EB/OL]. (2016-3-10). http://www.ncac.gwu.edu/vml/models.html.
[18] Standing Committee of the National People's Congress. (2003). Road Traffic Safety Law of the People's Republic of China. Gazette of the Standing Committee of the National People's Congress of the People's Republic of China, (6), 14.
[19] Mertz H J, Irwin A L, Prasad P. Biomechanical and scaling basis for frontal and side impact injury assessment reference values [J]. Stapp Car Crash J, 2016, 47 (10): 155-188.
[20] Takhounts E G, Craig M J, Moorhouse K, et al. Development of brain injury criteria (BrIC) [J]. Stapp Car Crash J, 2013, 57 (11): 243-66.